



Designing The Primary Nozzle Configuration of a Phase Change Ejector as an Expansion Device in the R134A Air-Water Heat Pump Cycle

Mohammed Ridha Jawad*, Wameedh T. Mohammed

Department of Mechanical Engineering, College of Engineering, University of Diyala, 32001 Diyala, Iraq

ARTICLE INFO

Article history:

Received October 23, 2024
Revised January 19, 2025,
Accepted January 30, 2025
Available online June 1, 2025

Keywords:

Phase change ejector
Design primary nozzle
Air to water heat pump cycle
Thermodynamic evaluation
Converging-diverging nozzle

ABSTRACT

The aim of this study is to develop a thermodynamic model for designing the primary nozzle (P-N) of a phase change ejector utilized in the Air - Water Heat Pump (AWHP) cycle. This expansion device is proposed to replace the conventional expansion devices with high irreversibilities losses in order to enhance the overall cycle efficiency. This simulation study is modelled using MATLAB software with REFPROP database used to obtain R134a thermodynamic properties. A comparison analysis of AWHP using valve, turbine or ejector as expansion devices is conducted. The ejector results is then used in the P-N design simulation. In addition, a sensitivity analysis to investigate the effects of varying R134a velocity at the P-N inlet on the design parameters is performed. The results show that ejector cycle has achieved higher COPh and second law efficiency by 3.25 and 6.6% respectively. In addition, the exergy evaluation demonstrates that using the ejector reduces the total exergy destruction by 51.7 and 48.5% compared to valve and turbine cycles respectively. The results also show that 20.7 J of exergy is destroyed in the ejector, of which 15.9 J of this destruction occurs in the P-N. The sensitivity analysis show that the P-N has a converging-diverging configuration with an inlet diameter ranging between 4.9-3.2 mm, while the throat diameter is between 3.11-2.7 mm and the outlet diameter is almost constant at 7mm. In addition, at the throat section, R134a reaches supersonic speed and highest mass flux and maintain the supersonic speed at the nozzle exit.

1. Introduction

Globally, the demand on energy supply and the associated environmental consequences are of major concerns. Many research have focused on developing new energy-saving technologies. A major sector of global energy production is consumed by domestic and industrial heating application and hence efforts have been made to improve the energy efficiency of heating systems. It is reported that expansion process is associated with significant irreversibility losses which in turn degrade the performance of the

conventional vapour compression heat pump system (VCHP) [1, 2]. It is therefore recommended to use low irreversible expansion devices such as heat exchanger [3], expander turbine [4], and phase change ejector [5].

Ejectors play vital roles in many industrial applications and show remarkable benefits in vapour compression refrigeration and heat pump cycles [6, 7]. Using the phase change ejector as an expansion device has shown significant enhancement in the coefficient of performance (COP) of the VCHP. It can draw the vapour refrigerant from the evaporator with

* Corresponding author.

E-mail address: mohammedridha_eng@uodiyala.edu.iq

DOI: [10.24237/djes.2025.18209](https://doi.org/10.24237/djes.2025.18209)

This work is licensed under a [Creative Commons Attribution 4.0 International License](https://creativecommons.org/licenses/by/4.0/).



no mechanical work required which consequently enhances the COP of this cycle [8]. Further advantages of using the phase change ejector include reducing evaporator size, higher expansion work recovery, low cost and low maintenance since it has no moving part [9].

The phase change ejector consists mainly of primary nozzle (P-N), secondary nozzle (S-N), mixing chamber (mix), constant area chamber and diffuser section (diff.) [10] as illustrated in Figure 1. Two thermal fluids (primary and secondary streams) will mix and exchange momentum in the ejector [11]. When the primary stream is liquid then the ejector is called two-phase ejector (2PHEJ) [12], alternatively, it is called steam injector when the motive stream is gas [13]. The primary fluid enters the ejector from the P-N inlet section where it expands isentropically to a pressure lower than the evaporator pressure at the mixing chamber section. This pressure drop entrains the vapour refrigerant to the mixing chamber with no consumption of compressor work. The most important part of the 2PHEJ is the primary nozzle where the expansion process of the refrigerant take place.

Although the ejector has a simple structure, the complexity of the thermodynamic process occurring on the refrigerant inside the ejector including flow speed change from subsonic to supersonic and phase change process require thorough investigation with particular attention to ejector design parameters [14]. The ejector design configuration and working boundary conditions, in particular the P-N configuration, including the diameters and refrigerant flow characteristics have a major effect on the ejector performance and consequentially the HP cycle, [15].

Numbers of simulation and experimental researches have studied the design and performance of the ejector as an expansion device in HP systems. Many working fluids have been investigated such as CO₂, R410A, R600a and R134a in both supercritical and subcritical cycles. An experimental study on VCHP with ejector is carried out to investigate the expansion of R134a without flux induction [15]. The experiment is conducted for a P-N pressure range between 7.7-16.8 bar and 30 °C

of subcooled degree. The main results from this study show that more P-N mass flow can be obtained at higher pressure and by subcooling the refrigerant at the P-N inlet section. Another experimental study investigated the ejector performance under different working conditions including P-N position relative to the mixing chamber section, P-N pressure between 8.8-14.9 bar and R134a subcooled degree of 0.2-5 °C [16]. The results show that the optimum position for the P-N is 38 mm from the mixing chamber. Both P-N inlet and outlet pressure have minimal effect on the entrainment ratio (below 10%). In contrast, subcooled degrees have increased the entrainment ratio by 66%. A comparison performance between the P-N converging nozzle and the converging-diverging nozzle is conducted experimentally [17]. This study concluded that higher primary nozzle mass flow and lower critical pressure at the throttling section are achieved in the converging nozzle. While higher entrainment ratio and lower throat diameter are achieved from the converging-diverging P-N configuration.

To better understand the flow parameter through the choking condition in the P-N of the two-phase ejector, an experimental study is conducted with no induction of R134a flow [18]. The results show that the effect of the slip ratio of vapour to liquid phase ranged between 13-23% on the compression ratio. While the impact on the throat diameters of the nozzle is 33-39%. Other studies have experimentally investigated the exergy analysis across the ejector to figure out the exergy efficiency and irreversibilities across each ejector section [19]. Compared with conventional VCC, the study supported that refrigeration cycle equipped with an ejector has lower irreversibility values by 5.9-12.6% and higher exergy efficiency by 6.7-14.2%. The effect of various geometrical factors on the performance of a phase change ejector using R290 is investigated experimentally [20]. The results show that the pressure lift ratio is dependent on the throat diameter and NXP (nozzle exit position) while the ejector length has minimal impact on the ejector performance. Numbers of published simulation studies in the literature have also investigated the design and performance of the phase change ejector. A one

dimensional (1D) thermodynamic model is proposed for designing the P-N of a two-phase ejector used in the CO₂ transcritical heat pump cycle [10]. CO₂ Ideal and non-ideal models have been proposed for comparison purposes. The results show that the P-N has a converging-diverging configuration and a shock wave has been detected at the diverging part of the P-N. The findings also support good agreement in the results between the two models regarding the refrigerant supersonic flow properties including Mach number, speed of sound and other design relations like velocity area relation. Another simulation comparison study found that only 4.4 watts of energy were destructed in the CO₂ heat pump ejector cycle compared to 9.4 and 13.4 watts were destructed in turbine expander and expansion valve cycles respectively under the same working conditions [21]. Using the same working fluid of CO₂, another comparison study found that the ejector cycle has lower exergy destruction compared to turbine and expansion valve cycles by 59% and 71% respectively [22].

More simulation studies have been proposed for designing and investigating the phase change ejector. A study has modelled thermodynamically the two-phase ejector of the 5-kW refrigeration cycle in terms of the main ejector configuration sections including P-N throat and outlet diameters [23]. In this study, more geometrical aspects have been involved such as secondary nozzle and mixing chamber diameters to investigate the cycle performance under various working conditions. The nominated refrigerants used in this study are R1234yf, R1234ze (E), and R134a. The results show that the P-N throat diameter is increased as condensation temperature increases. In addition, P-N outlet diameter is highly dependent on the evaporation temperature and the working boundary conditions.

Additional applications for the ejector have been proposed recently for the two-phase ejector such as water condensation through the expansion process. A numerical investigation using a 2D CFD model is performed to investigate the condensation of pure H₂O in one case study and a mixture of H₂O and CO₂ gas in another scenario [24]. The condensation

process takes place through the expansion process in a two-phase ejector under various working conditions. The main result revealed that reducing the inlet ejector pressure causes lower steam entrainment ratio, mixture velocity and exit temperature. In addition, it has been noticed that in the mixture case, higher inlet pressure is required due to the higher mixture density. Another research have designed a simple thermodynamic model to simulate the ejector performance in refrigeration or power generation cycles using R141b as the working fluid [25]. An empirical mathematical correlation has been proposed to predict the primary nozzle entrainment and compression ratios across the nozzle which achieved an accuracy of 8.4% and 6.3% respectively compared to experimental results adopted from the literature. Another one-dimensional simulation model is developed [26]. The model was validated under steady working conditions with experimental results and benchmarked with a 2D CFD model under variable working conditions for further calibration. The results show that the model shows good prediction of flow momentum and mass flow rate for various working conditions.

Further application of the two-phase ejector has been extended to include more thermodynamic cycles. The performance of the ejector condenser in a gas power plant has been investigated [27]. The main task of the ejector in this application is to entrain and condense the vapour in the flow of exhaust gases. The ejector geometry and the presence of CO₂ in the exhaust flow gases are also involved in the analysis of this study. The CFD simulation results show that the condensation process is intensive in the suction nozzle and the presence of CO₂ has reduced the rate of condensation. Another 3D CFD model is developed to study the condensation of water and steam with existing non-condensable gases in the two-phase ejector [28]. The presence of these gases reduces the condensation heat transfer by preventing the direct contact between the water and steam which can cause damage to the equipment. The results reveal that increasing the steam inlet pressure improves the heat transfer coefficient. However, when the mass fraction of

the non-condensable gases increased by 1-10%, a lower heat transfer coefficient between water and steam has been recorded.

In current study, a one-dimensional thermodynamic model is developed to investigate the expansion process in the P-N of a two-phase ejector in a heat pump cycle. This HP cycle is combined with an Organic Rankine cycle (ORC) for heating applications is adopted from previous work [29]. R134a thermophysical properties in steady-state mode is calculated and the outcome is used as a boundary condition for designing the ejector P-N. Others thermophysical properties such as density, quality, internal energy, mass flux and supersonic flow characteristics including Mach number and speed of sound are evaluated during the expansion process. Moreover, the main

geometrical design parameters are obtained including the P-N contour and the main P-N diameters. The results are validated with experimental studies available in the literature.

2. Thermodynamic concepts, assumptions, boundary conditions and mathematical model.

The proposed heat pump cycle is assumed to be mechanically powered by the ORC cycle which is thermally driven by a gas burner. This combined system is designed to provide hot water for heating applications [30]. The assumptions and working conditions in this study are adopted to meet the design requirement of this combined system.

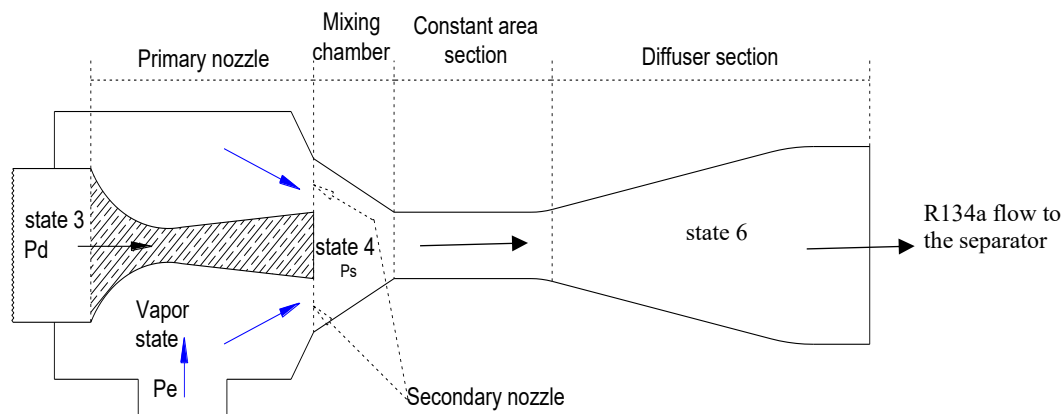


Figure 1. Schematic of an Ejector [10].

The evaluation focuses on the Air-to-Water Ejector Heat Pump cycle (AWEHP) which is designed to pump ambient thermal energy to heat tap water as shown in Figure 2. The saturated liquid refrigerant enters the ejector from the condenser exit and expands through the P-N as shown in State 3-4 PH and TS diagrams in Figure 3. This expansion will create a vacuum pressure zone at the P-N exit (State 5), which will entrain the vapour refrigerant from the evaporator exit (State 9) to the mixing chamber without consuming mechanical energy. The two fluids are mixed and exchange momentum in the mixing chamber and a further increase in the pressure is achieved at the ejector exit (State 6) as shown in Figure 3. MATLAB software is

used to develop the mathematical mode. The thermophysical properties of R134a are acquired from the REFPROP database [31].

2.1 Assumption and boundary conditions

The main assumptions adopted in the modelling procedure are:

1. Constant pressure mixing approach is adopted which is preferable for the entrainment process of the secondary stream [6].
2. R134a as a saturated liquid enters the ejector P-N at a constant pressure of 815.42 kPa and a temperature of 32 °C.

3. R134a enters the P-N at low velocity ranged between 0.1-0.5 m/s.
4. The isentropic efficiency for the P-N ejector and compressor are 85% and 80% respectively, which are adopted from the literature [32].
5. Pinch point temperature of 3 °C between the refrigerant and the ambient air stream is assumed at the evaporator. The lowest ambient air temperature is set to 5.5 °C, hence, the evaporation temperature and pressure are set as 2.5 °C and 320.26 kPa, respectively.
6. R134a is superheated by 3 °C at the compressor inlet to avoid the saturated mixture zone.
7. The pressure drop across entire HP ejector cycle can be neglected due to its minimal values compared with other conventional cycles. This assumption is validated experimentally [33].

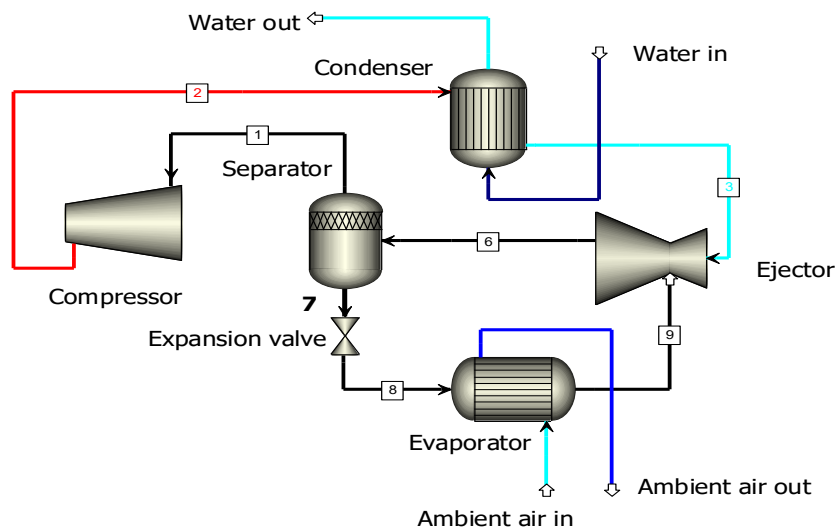


Figure 2. Air to water Ejector Heat pump cycle

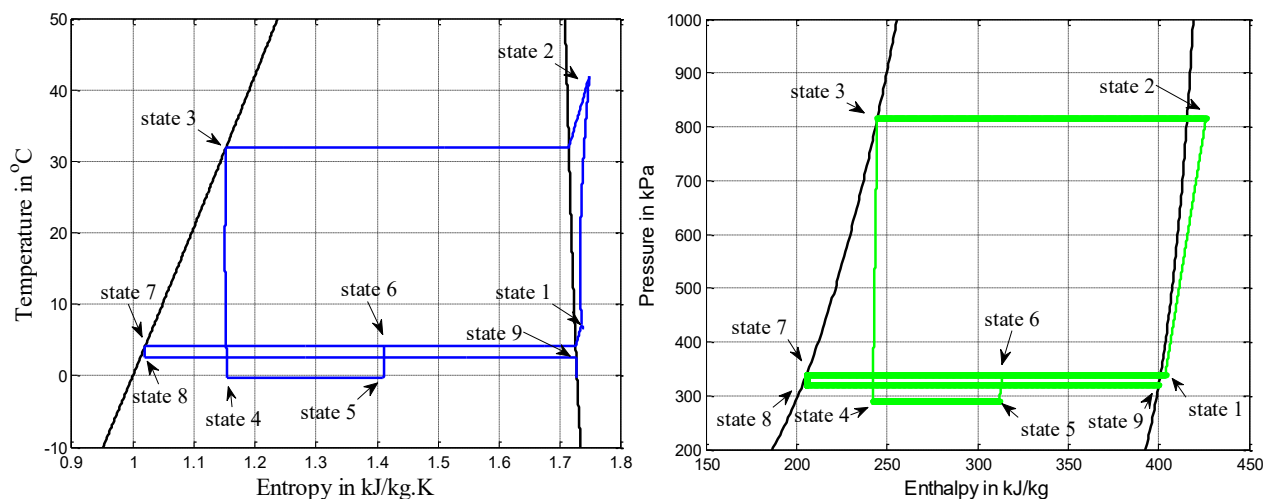


Figure 3. PH and TS diagrams for Air to water Ejector Heat pump cycle

2.2 Mathematical model

The mathematical equations used in this study are adopted from the following references [10, 21-22].

The coefficient of performance for the HP ejector cycle is calculated as follow:

$$COP_h = \frac{h_2 - h_3}{h_2 - h_1} \quad (1)$$

This equation is also applied on the valve and turbine HP cycles taking in consideration the corresponding difference in enthalpy states across condenser and compressor for each cycle. The second law efficiency equation is:

$$\text{second law efficiency} = \frac{COP_h}{1 - (T^8/T_3)} \quad (2)$$

The exergy destruction for the expansion devices is calculated as follow:

The general form of exergy destruction is:

$$I = T_o \times m_{R134a} \times \Delta S \quad (3)$$

Exergy destruction for ejector:

$$I_{ejector} = \sum I_{P-N} + I_{S-N} + I_{mix.} + I_{diff.} \quad (4)$$

While;

$$I_{P-N} = T_o m_p (S_4 - S_3) \quad (5)$$

Where T_o is the reference temperature, m_p is the primary mass flow across the P-N.

The energy formula for 1-D steady state adiabatic flow is:

$$h_3 - h_4 = \frac{u_4^2}{2} - \frac{u_3^2}{2} \quad (6)$$

Where u and h are the refrigerant velocity and enthalpy at a specific state respectively.

By assuming variable inlet velocity at P-N inlet,

$$u_4 = \sqrt{u_3^2 + 2(h_3 - h_4)} \quad (7)$$

The speed of sound is calculated form the following equation:

$$c = \sqrt{\frac{c_p}{c_v} \times \frac{\Delta P}{\Delta \rho}} \quad (8)$$

The equation of Mach number is below:

$$Mach = \frac{u}{c} \quad (9)$$

The two main converging-diverging nozzle design equations are listed below:

$$\frac{dA}{A} = -\frac{dv}{v} (1 - Mach^2) \quad (10)$$

$$\frac{A}{A^*} = \frac{1}{Mach} \left[\left(\frac{2}{k+1} \right) \left(1 + \frac{k-1}{2} Mach^2 \right) \right]^{\frac{(k+1)}{2(k-1)}} \quad (11)$$

3. Results and discussion

3.1 Steady state results

Table 1 shows the calculated steady state results of pressure, temperature, enthalpy and entropy for R134a at different states across the ejector HP cycle which has been demonstrated graphically in the TS and PH diagrams (Figure 2).

Table 2 shows efficiency performance comparison for the Air - Water Heat Pump cycle (AWHP) using three expansion devices namely, conventional valve, turbine expander and two-phase ejector. The results show that ejector cycle has achieved higher COP_h and second law efficiency compared to turbine expander and valve cycles by 3.25 and 6.6% respectively.

3.2 Exergy analysis for Air - Water Heat Pump cycle using different expansion devices

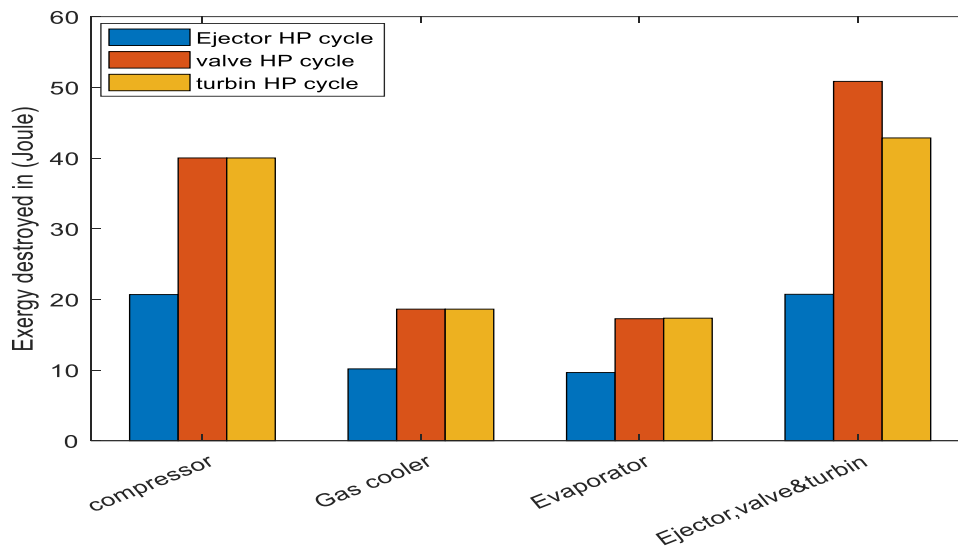
Figure 4 compares the amount of exergy destroyed in the main components of Air - Water Heat Pump cycles namely, compressor, condenser, evaporator and expansion device. In the compressor, the exergy destroyed is around 40 J for HP turbine and valve cycles, while in the HP ejector cycle, the compressor has destroyed only around 20 J. In the condenser and evaporator, the amount of exergy destruction for HP valve and turbine cycles are similar and equal to 18.6 and 17.3 J respectively. While for HP ejector cycle, only around 10 J of exergy is destroyed in the condenser and evaporator. Meanwhile, the total exergy destroyed during the expansion process is higher in the valve and turbine cycles with values of 50.83 and 42.83 J respectively. In contrast, the two-phase ejector has the lowest exergy destruction of 20.7 J. Overall, using the ejector in the HP cycle reduces the total exergy destructed by 51.7 and 48.5% compared to expansion valve and turbine HP cycle respectively.

Table 1: Thermophysical properties of R134a at different states across the entire HP ejector cycle

| States | Pressure in kPa | Temperature in °C | Enthalpy in kJ/kg | Entropy in kJ/kg.K |
|--------|-----------------|-------------------|-------------------|--------------------|
| 1 | 339.13 | 7.27 | 403.73 | 1.734 |
| 2 | 815.426 | 42.016 | 426.19 | 1.7474 |
| 3 | 815.426 | 32 | 244.62 | 1.144 |
| 4 | 290.2635 | -0.2402 | 242.16 | 1.15 |
| 5 | 290.2635 | -0.2402 | 398.358 | 1.72 |
| 6 | 339.1363 | 4.1243 | 311.92 | 1.41 |
| 7 | 339.1363 | 4.1243 | 314.03 | 1.411 |
| 8 | 320.2635 | 2.5 | 314.03 | 1.413 |
| 9 | 320.2635 | 2.5 | 400.05 | 1.725 |

Table 2: Comparison between the COP_h and the exergy efficiency for HP with three expansion devices

| Parameters | HP Expansion valve cycle | HP Turbine expander cycle | HP Ejector cycle |
|-----------------------|--------------------------|---------------------------|------------------|
| COP _h | 7.5989 | 7.8454 | 8.1005 |
| Second law efficiency | 73.4974 | 75.8816 | 78.3495 |


Figure 4. Exergy destruction across different components of the AWHP using three expansion devices

3.3 Effects of expansion process across the P-N on R134a thermophysical properties and flow characteristics.

Figure 5 illustrates the effects of R134a expansion across the P-N on the refrigerant quality. As shown in the Figure, R134a entered the P-N as almost fully saturated liquid ($X=0.12$). It then changes into a two-phase flow during the expansion process. The overall refrigerant phase changes take place when the pressure ranged between 290.2-396.3 kPa. At the P-N exit, R134a leaves with a quality of 21.5%.

The exergy destruction and the entropy change of R134a across the P-N during the expansion process are displayed in Figure 6. The results show that as the refrigerant expands from 800-300 kPa, the exergy destruction increases. However, only around 0.0159 kJ of exergy is destroyed. This can be explained by the low entropy generated during the expansion process ($\Delta s = 0.0097$ kJ/kg.K). Hence, this design has achieved nearly isentropic expansion of the refrigerant.

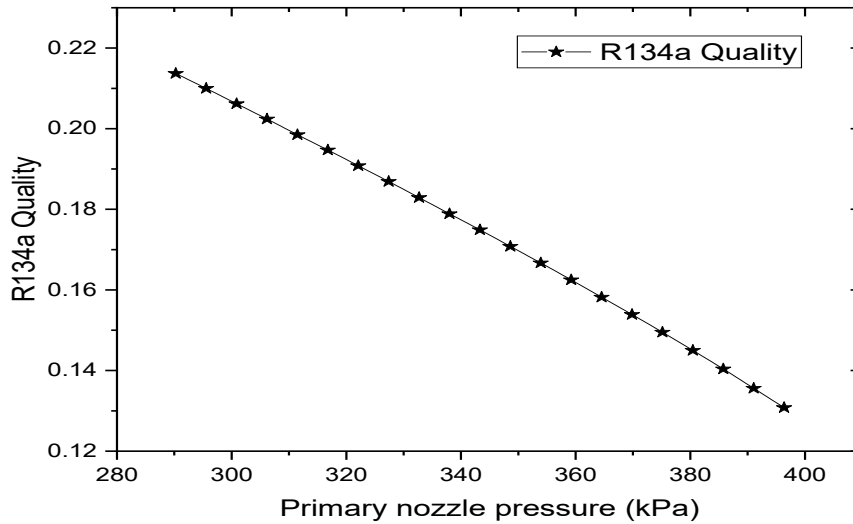


Figure 5. R134a quality during the expansion process in the P-N.

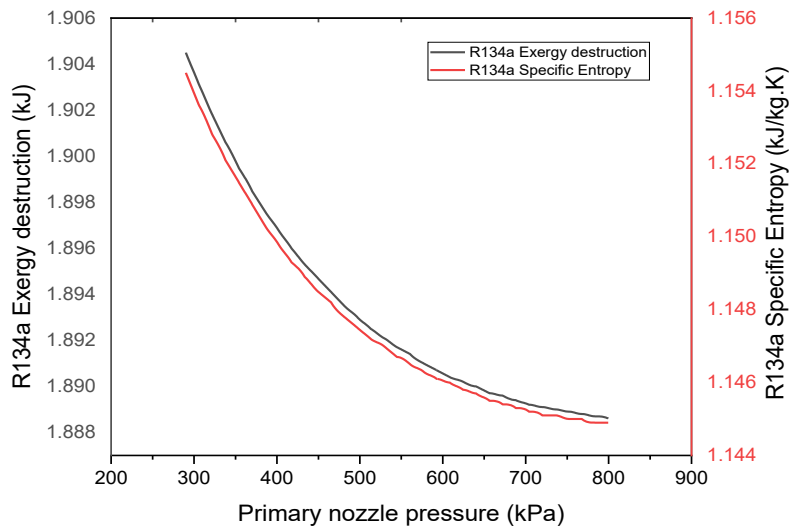


Figure 6. Exergy destruction and entropy change during the expansion process.

The results also show that the main exergy destruction in the two-phase ejector take place in the P-N section (15.9 out of 20.7 J (Figure 4)).

Figure 7 explains the effects of the expansion process on the internal energy and the specific volume of R134a. Through the converging part, these thermodynamic properties maintain constant values up to the throat section. At this point, the internal energy record the highest value of 241.5 kJ/kg then declines through the diverging part up to the exit section. While the specific volume of R134a

increases from the lowest value at a throttling pressure of 751.77 kPa to reach the maximum at the nozzle exit. Both properties behaviour confirms the typical expansion process of gases inside a converging-diverging nozzle.

In Figure 8, R134a density has shown no significant change at the converging part of the nozzle which proves that the flow is incompressible. While at the diverging part of the P-N, the density declines to indicate that R134a flows in a compressible manner.

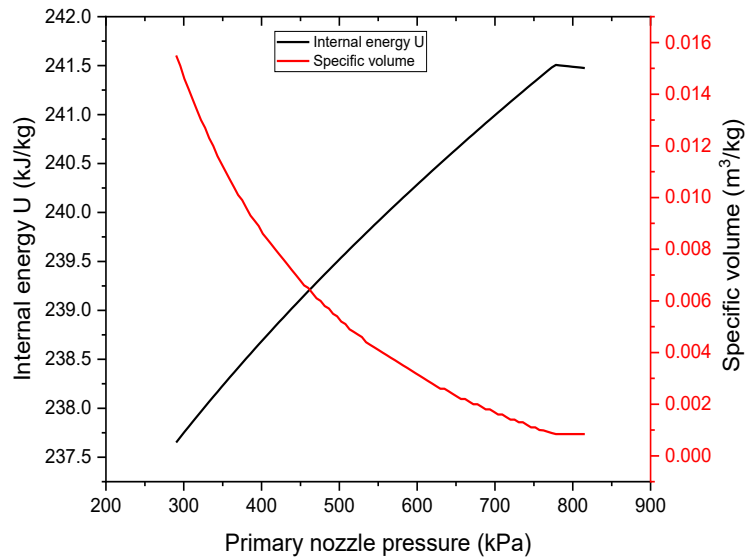


Figure 7. Primary nozzle pressure correlation internal energy and specific volume

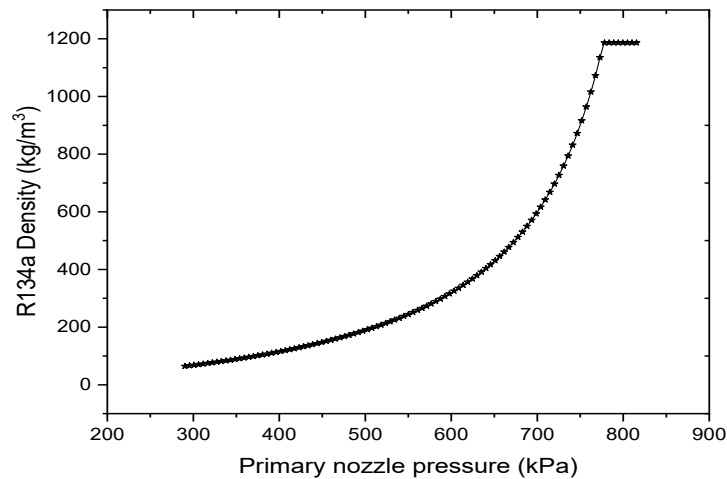


Figure 8. R134a density variation during the expansion process.

3.4 Sensitivity analysis for varying the refrigerant velocity at the P-N inlet.

In this section, the impacts of varying R134a velocity at the inlet of the P-N on the design parameters and the refrigerant thermophysical properties are investigated and discussed.

Figure 9 shows the 3D contour of the P-N at different R134a inlet velocities. As shown, the mathematical model has predicted the shape of the P-N as a converging-diverging nozzle in all selected velocities. It also demonstrates the P-N inlet diameter significantly depends on the refrigerant inlet velocity which has less impact on the throat and exit diameters of the P-N.

Figure 10 shows the P-N diameter correlation with the pressure at different R134a inlet velocities (U_3). The refrigerant expands from a pressure value of 810 to 290 kPa. As the initial refrigerant velocity increased from 0.1 - 0.5 m/s, the inlet diameter decreased from 4.9-3.2 mm. While the throat diameters decreased from 3.11-2.7 mm. In contrast, the outlet diameter minimally changed from 7.0-6.94 mm. Figure 11 shows the behaviour of mass flux during the expansion process in the P-N for different R134a inlet velocities. As the pressure declines to throttling pressure, the mass flux increases significantly to reach its maximum values of 725.4 kg/m².S for inlet velocity of 0.1 m/s and up to 917.2 kg/m².S at a velocity of 0.5 m/s. After the refrigerant passes the P-N throat

area, the mass flux declines significantly to reach its lowest values (between 142.8-146.2 kg/m².S) at the P-N outlet.

Figure 12 shows the velocity of R134a during the expansion process for different inlet velocity. As the refrigerant passes through the primary nozzle, its velocity significantly increases to reach its highest value at the P-N outlet. In addition, the R134a velocity at the nozzle exit is nearly equal (approximately 2.3 m/s) despite the various refrigerant inlet velocities.

Figure 13 shows the relation between the refrigerant Mach number and nozzle pressure at different R134a inlet velocities. The results show that for all selected velocities, the Mach number increased significantly from subsonic speed (M<1) at the converging part of the nozzle to reach a supersonic speed at the throat section. In addition, increasing the refrigerant inlet velocity produces higher Mach numbers at the P-N throat pressure. At the exit section, the refrigerant leaves the nozzle with a velocity higher than the speed of sound with minimal impact of the R134a inlet velocity.

Figure 14 shows the area velocity correlation ($\frac{dA}{dV}$) in terms of Mach number in the supersonic speed domain of the converging-

diverging nozzle. It is known that $\frac{dA}{dV}$ relation governs the configuration of the converging-diverging nozzle during the expansion process. When $\frac{dA}{dV} < 0$, it indicates the flow is subsonic, while $\frac{dA}{dV} = 0$ means sonic speed flow and for $\frac{dA}{dV} > 0$, the flow is supersonic. The result shows that as the Mach number increases, the $\frac{dA}{dV}$ in the diverging part of the P-N section has a positive value which indicates that the diverging section has secure supersonic speed at the P-N exit. The variations in the R134a inlet velocity have minimal impact on the $\frac{dA}{dV}$ at throat section while the ratio increases toward the nozzle exit with a slight difference in the $\frac{dA}{dV}$ values of 49.5-53.4 at inlet velocity of 0.1-05 m/s, respectively.

Figure 15 demonstrate the relation between the nozzle area ratio ($\frac{A}{A^*}$) and the Mach number. The area ratio represents the local area at each Mach number over the throttling area section. The results present only the diverging part of the nozzle. At the throat section when Mach number is maximum, the area ratios are unity for all selected refrigerant inlet velocities. After that the area ratio increases to reach its maximum values at the P-N exit.

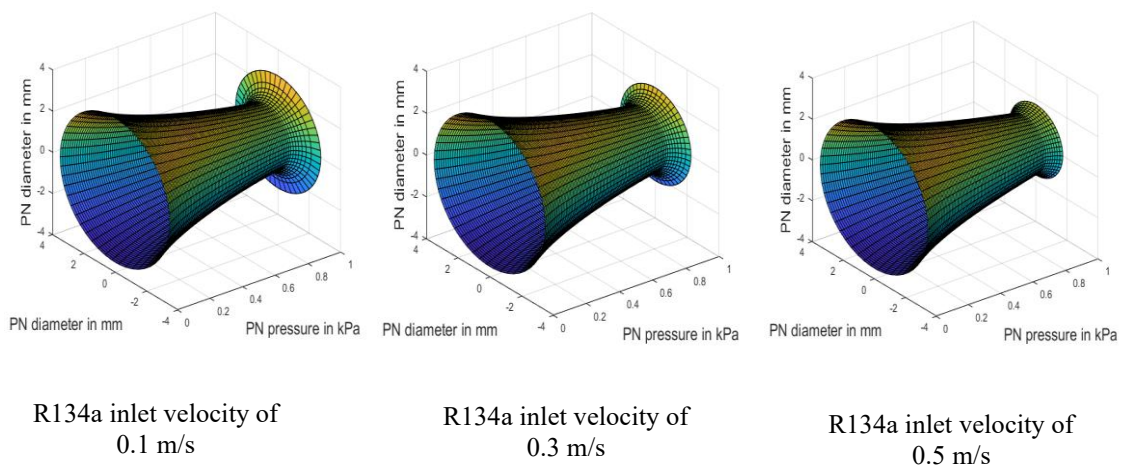


Figure 9. 3D domain of primary nozzle

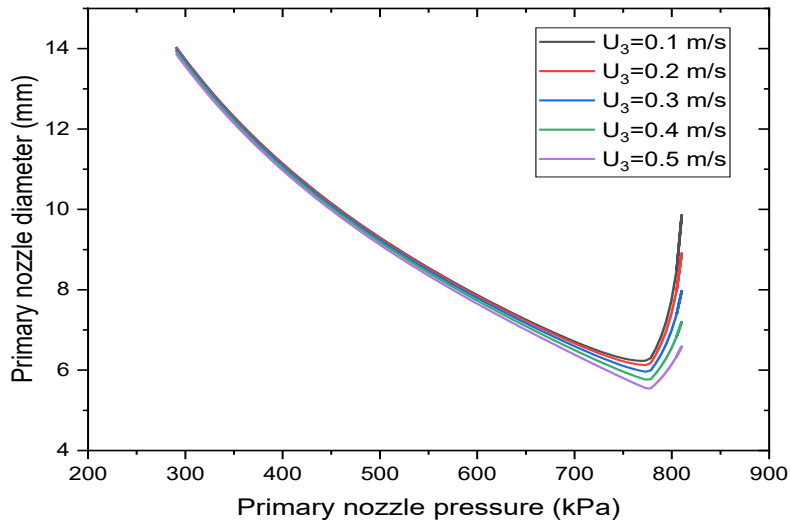


Figure 10. Sensitivity analysis of P-N diameters with R134a inlet velocities

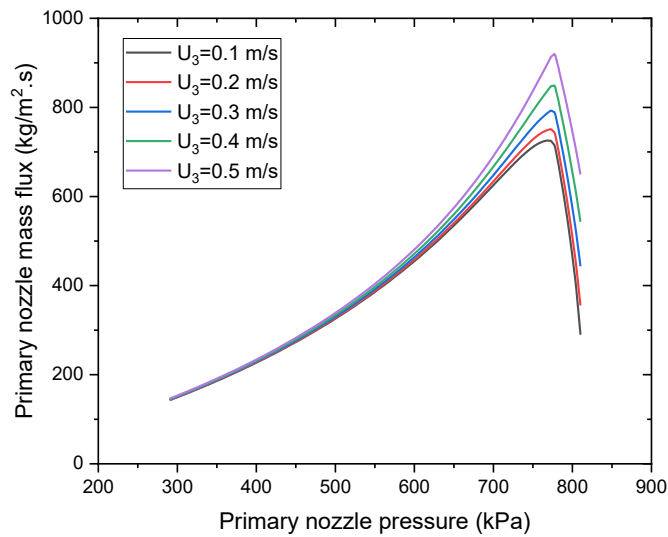


Figure 11. Sensitivity analysis of P-N mass flux with R134a inlet velocities

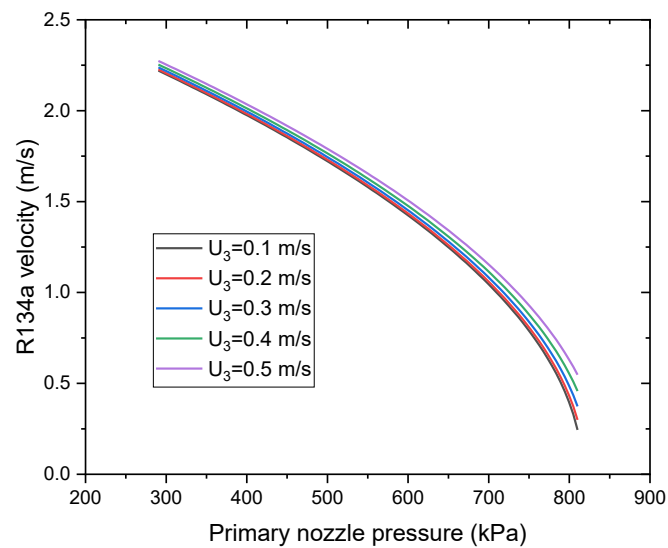


Figure 12. Sensitivity analysis R134a velocities during the expansion process

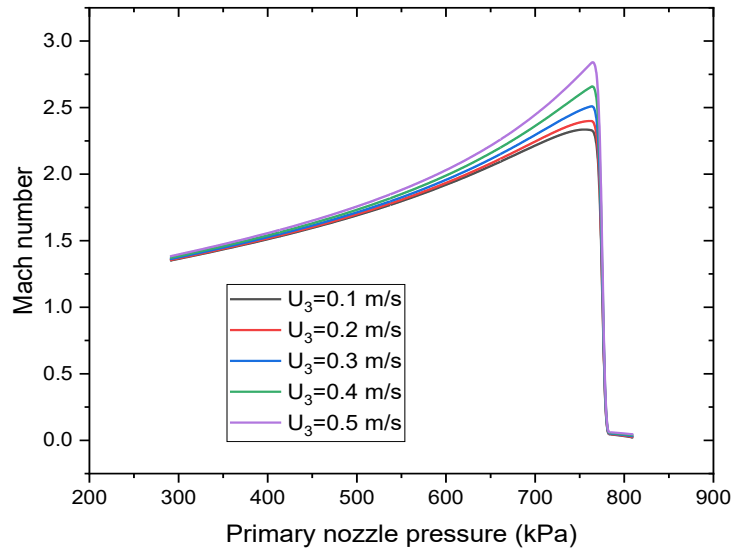


Figure 13. Sensitivity analysis of Mach number with R134a inlet velocities

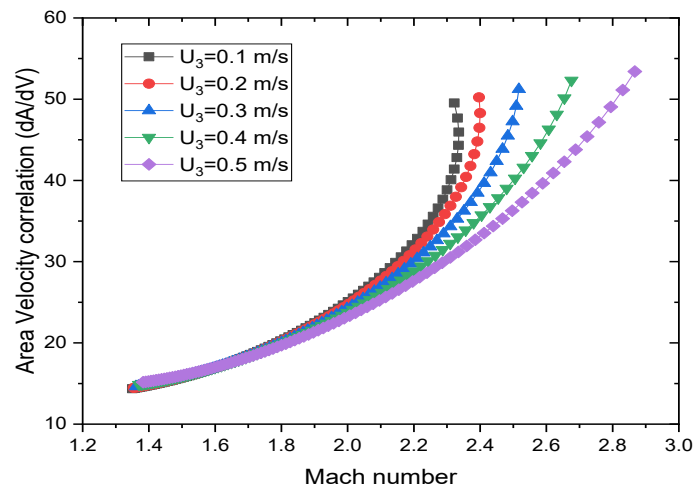


Figure 14. Sensitivity analysis of area velocity relation and Mach number for different R134a inlet velocities

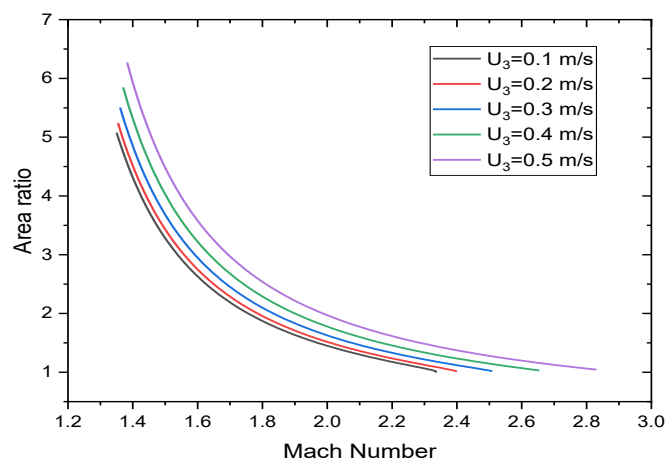


Figure 15. Sensitivity analysis of area ratio and Mach number for different R134a inlet velocities

4. Validation of current work with the experimental studies

To the best of the author's knowledge, there is lack of experimental studies that adopts similar boundary conditions and working assumptions used in the current study. These boundary conditions satisfy the design requirement for the combined HP-ORC system [30]. Hence the results of current study are compared and validated against experimental studies by K. Ameer and Z. Aidoun [16] and K. Ameer, Z. et al [17] which adopt similar thermodynamic concepts and use the same working fluid (R134a). In these experimental studies, the condenser pressure at the P-N inlet ranged between 880-1490 kPa compared to the current study which has a constant value of 815.4 kPa. In addition, the nozzle exit position (NXP), nozzle length and the divergence and convergence angles are not considered in the current study. Furthermore, the refrigerant is subcooled by 0.2-5 °C in these studies. The ejector outlet pressure of 340 kPa was in close agreement with the experimental results (370-470 kPa). The nozzle used in the experimental studies has inlet, throat and exit diameters of 10, 1.39 and 4 mm, respectively. In the current study, these parameters varied according to the refrigerate inlet velocity. For instant, at refrigerant velocity of 0.1 m/s, the P-N inlet, throat and exit diameters are 4.92, 3.1 and 7 mm respectively. Only the inlet and throat diameters decreases when the velocity increased to 0.5 m/s (3.3 mm inlet and 2.8 mm throat diameters). In addition to the above mentioned reasons, the differences between the current simulation study and the experimental studies can be attributed to the limitation of 1D analysis.

5. Conclusions

A one-dimensional thermodynamic model is developed to design the primary nozzle of an ejector in the AWHP cycle. MATLAB software is used and the thermophysical properties of the refrigerant are acquired from the REFPROP software. The results show the two-phase ejector used as an expansion device has improved the cycle COPh and the second law efficiency by 3.25 and 6.6% compared to

conventional valve and turbine expander HP cycle respectively. In addition, the exergy destroyed during the expansion process is 50.83, 42.83 and 20.7 J for valve, turbine and ejector cycles correspondingly. The overall exergy destruction in the ejector HP cycle is around 50% lower than HP cycle with the other expansion devices. In addition, most of the exergy destroyed during the expansion process in the ejector device occurs in the P-N accounting for around 73%. Moreover, R134a undergoes a phase change during the expansion process and leave the P-N with a quality of 21.5%. The sensitively analysis of changing R134a inlet velocity between 0.1-0.5 m/s show that the P-N inlet diameter ranged between 3.2-4.9 mm and the throat diameter decreased as the inlet velocity increased with a value of 3.11-2.7 mm while the outlet diameter remains constant at around 7mm. The refrigerant mass flux and Mach number peaked at the throat section. Moreover, during the expansion of R134a in the P-N, only 0.0097 kJ/kg.K of entropy is generated, which indicates the P-N design has achieved high isentropic efficiency. In addition, refrigerant density values indicate that the flow is compressible. The ratio $\frac{dA}{dV}$ in the diverging part of the P-N have achieved positive values which indicate the refrigerant exit the nozzle with supersonic speed ($M > 1$). The current study provide a primary approach for designing the P-N of a phase change ejector. However, further investigations to involve more design parameters such as NXP, nozzle length and angles of convergence and divergence are required. Also, due to the limitation of the 1D model, future work to include 2D modelling using CFD software as well as experimental work is recommended.

References

- [1] K. Sutthivirode, T. Thongtip, "Experimental investigation of a two-phase ejector installed into the refrigeration system for performance enhancement," *Energy Reports*, vol. 8, pp. 7263-7273, Jun. 2022.
- [2] T. Bai, Y. Lu, J. Wan and J. Yu, "Experimental investigation on the malfunction characteristics of the two-phase ejector in a typical enhanced refrigeration system," *Applied Thermal Engineering*, vol. 262, Mar. 2024.

- [3] T. Bai, G. Yan, J. Yu, "Influence of internal heat exchanger position on the performance of ejector-enhanced auto-cascade refrigeration cycle for the low-temperature freezer," *Energy*, vol, 238, Part C, Jan. 2022.
- [4] M.T. Erdinc, "Two-evaporator refrigeration system integrated with expander-compressor booster," *International Journal of Refrigeration*, vol. 154, pp. 349-363, Oct. 2023.
- [5] S.K. Yadav, K. Murari Pandey, R. Gupta, "Recent advances on principles of working of ejectors: A review," *Materials Today: Proceedings*, vol. 45, Part 7, pp. 6298–6305, 2021.
- [6] Z. Aidoun, K. Ameer, M. Falsafioon, M. Badache, "Current Advances in Ejector Modeling, Experimentation and Applications for Refrigeration and Heat Pumps. Part2: Two-Phase Ejectors," *Inventions*, vol. 4 (1), Mar. 2019.
- [7] G. Toffoletti, R. B. Barta, S. M. Grajales, H. Liu, D. Ziviani, E. A. Groll, "Experimental Comparison of Cycle Modifications and Ejector Control Methods Using Variable Geometry and CO2 Pump in a Multi-Evaporator Transcritical CO2 Refrigeration System," *International Journal of Refrigeration*, vol. 169, pp. 226-240, Jan. 2025.
- [8] G. Toffoletti, R. B. Barta, S. M. Grajales, H. Liu, D. Ziviani, and E. A. Groll, "Experimental comparison of cycle modifications and ejector control methods using variable geometry and CO2 pump in a multi-evaporator transcritical CO2 refrigeration system," *International Journal of Refrigeration*, vol, 169, pp. 226-240, Oct. 2024.
- [9] H. Ding, Y. Dong, Y. Yang and C. Wen, "Performance and energy utilization analysis of transcritical CO2 ejector considering non-equilibrium phase changes," *Applied Energy*, vol. 372, Oct. 2024.
- [10] M. R. J. Al-Tameemi and Z. Yu, "Thermodynamic approach for designing the two-phase motive nozzle of the ejector for transcritical CO2 heat pump system," *Energy Procedia*, vol. 142, pp. 1206-1212, Aug. 2017.
- [11] A. M. Hussien, W. H. Al Doori, "Modification in Parameters Affecting Ejector Flow Performance in the Condenser of Thermal Power Plants," *International Journal of Energy Conversion*, vol. 12, pp. 32-39, Apr. 2024.
- [12] N. Lawrence, S. Elbel, "Mathematical modeling and thermodynamic investigation of the use of two-phase ejectors for work recovery and liquid recirculation in refrigeration cycles," *International Journal of Refrigeration*, vol. 58, pp. 41-52, Oct. 2015.
- [13] H. Ma, H. Zhao, L. Wang, Z. Yu, X. Mao, "Modeling and investigation of a steam-water injector," *Energy Conversion and Management*, vol, 151, pp, 170-178, Nov. 2017.
- [14] L. Zheng, Y. Zhang, L. Hao, H. Lian, J. Deng, W. Lu, "Modelling, Optimization, and Experimental Studies of Refrigeration CO2 Ejectors: A Review," *Mathematics*, vol. 10, Nov. 2022.
- [15] K. Ameer, Z. Aidoun, M. Ouzzane, "Expansion of subcooled refrigerant in two-phase ejectors with no flux induction," *Experimental Thermal and Fluid Science*, vol. 82, pp. 424-432, Apr. 2017.
- [16] K. Ameer, Z. Aidoun, "Nozzle Displacement Effects on Two-Phase Ejector Performance: An Experimental Study," *Journal of Applied Fluid Mechanics*, vol. 11, pp. 817-823, Jan. 2018.
- [17] K. Ameer, Z. Aidoun, M. Falsafioon, "Experimental Performance of a Two-Phase Ejector: Nozzle Geometry and Subcooling Effects," *Inventions*, vol. 5, Jun. 2020.
- [18] K. Ameer, Z. Aidoun, M. Ouzzane, "Analysis of the Critical Conditions and the Effect of Slip in Two-Phase Ejectors," *Journal of Applied Fluid Mechanics*, vol, 9, pp. 213-222, Feb. 2016.
- [19] N. B. Sağ and H. K. Ersoy, A. Hepbasli, "An experimental investigation on exergy analysis of an ejector expansion refrigeration system", *International Journal of Exergy*, vol, 24, pp. 201-215, Oct. 2017.
- [20] Y. Lu, T. Bai and J. Yu "Investigation on the influence of geometric parameters on two-phase ejector performance with R290," *International Journal of Refrigeration*, vol, 156, pp. 102-112, Aug. 2023.
- [21] M. R. J. Al-Tameemi, Z. Yu, P. Younger, "Numerical investigation of the transcritical CO2 heat pump system employing different expansion devices," *12th IIR Gustav Lorentzen Natural Working Fluids Conference*, Edinburgh, 2016, pp. 66-73.
- [22] M. R. J. Al-Tameemi, K. N. Abed, T. K. Salem, Z. Yu, "Thermodynamic analysis with energy recovery comparison of transcritical CO2 heat pump system using various expansion devices," *Engineering Sciences (ISCES 2020) 16th-17th December 2020, Diyala, Iraq*.
- [23] A. U. Atmaca, A. Ereğ, O. Ekren, "Preliminary Design of the Two-Phase Ejector under Constant Area Mixing Assumption for 5 kW Experimental System," *4th International Conference on Advances on Clean Energy Research (ICACER 2019), Coimbra, Portugal, April 5-7, 2019*.
- [24] T. Ku's and P. Madejski, "Numerical Investigation of a Two-Phase Ejector Operation Taking into Account Steam Condensation with the Presence of CO2," *Energies*, vol. 17, May 2024.

- [25] H. A. Muhammad et al, "Numerical Modeling of Ejector and Development of Improved Methods for the Design of Ejector-Assisted Refrigeration System," *Energies*, vol. 13, Nov. 2020.
- [26] J. V. d. Berghe, B. R. B. Diasa, Y. Bartosiewicz, M. A. Mendez, "A 1D Model for the Unsteady Gas Dynamics of Ejectors," *Energy*, vol. 267, Mar. 2023.
- [27] Tomasz Kuś and Paweł Madejski, "Analysis of the Multiphase Flow With Condensation in the Two-Phase Ejector Condenser Using Computational Fluid Dynamics Modeling", *Journal of Energy Resources Technology*, vol. 146, Jan. 2024.
- [28] Y. Chai, et al, "Numerical Simulation on Two-Phase Ejector with Non-Condensable Gas," *Energies*, vol. 17, Mar. 2024.
- [29] M. R. J. Al-Tameemi, Y. Liang and Z. Yu, "Design Strategies and Control Methods for a Thermally Driven Heat Pump System Based on Combined Cycles," *Frontiers in Energy Research*, vol. 7, Nov. 2019.
- [30] Y., M. Al-Tameemi, Z. Yu, "Investigation of a gas-fuelled water heater based on combined power and heat pump cycles," *Applied Energy*, vol. 212, pp. 1476-1488, Feb. 2018.
- [31] Lemmon, E. et al, "NIST Reference Fluid Thermodynamic and Transport Properties Database (REFPROP), Version 9.1.
- [32] Md. E. Ahammed, S. Bhattacharyya, M. Ramgopal, "Thermodynamic design and simulation of a CO₂ based transcritical vapour compression refrigeration system with an ejector," *International Journal of Refrigeration*, vol. 45, pp. 177-188, Sep. 2014.
- [33] H. K. Ersoy and N. B. Sag, "Preliminary experimental results on the R134a refrigeration system using a two-phase ejector as an expander". *International Journal of Refrigeration*, vol. 43, pp. 97-110, Apr., 2014.